Preventing the oil film instability in rotor-dynamics

F Sorge

DICGIM, Polytechnic School of Palermo University, 90128 – Palermo, Italy

francesco.sorge@unipa.it

Abstract. Horizontal rotor systems on lubricated journal bearings may incur instability risks depending on the load and the angular speed. The instability is associated with the asymmetry of the stiffness matrix of the bearings around the equilibrium position, in like manner as the internal hysteretic instability somehow, where some beneficial effect is indeed obtainable by an anisotropic configuration of the support stiffness. Hence, the idea of the present analysis is to check if similar advantages are also obtainable towards the oil film instability. The instability thresholds are calculated by usual methods, such as the Routh criterion or the direct search for the system eigenvalues. The results indicate that the rotor performances may be improved in the range of low Sommerfeld numbers by softening the support stiffness in the vertical plane, and hardening it on the horizontal one, up to the complete locking, though this advantage has to be paid by rather lower instability thresholds for large Sommerfeld numbers. Nevertheless, a "two-mode" arrangement is conceivable, with some vertical flexibility of the supports for large journal eccentricity, and complete locking for small eccentricity. As another alternative, the support anisotropy may be associated with the use of step bearings, whose particular characteristic is to improve the stability for small eccentricities.

1. Introduction

The oil film journal bearings are often present in rotating machinery and lead to whirl instability on increasing the rotational speed over certain critical levels, requiring the use of limit pads or adequate damping sources of external origin. Several wide-ranging treatises deal with these and similar problems in the literature on rotor-dynamics (see [1-2] for example). Moreover, a great number of papers address the dynamical characteristics of lubricated journal bearings in order to formulate the reaction forces by proper stiffness and damping matrices, in the hypothesis of small displacement from the equilibrium configuration. A very comprehensive survey on this matter may be found in [3].

More recent trends of the research on the dynamics of journal bearings address new aspects that have received increasing attention in the last decades, such as the nonlinear characteristics of the mutual forces between the journals and the bearings in those dynamical conditions where the relative displacement between the two sliding members of the pair, though within the admissible range, has a non-negligible order of magnitude if compared with the clearance. For example, references [4-8] try to identify nonlinear coefficients for the functional expression of the forces being exchanged through the oil film, using various numerical or semi-analytical methods. The effects on the journal bearings behaviour of neighbouring seals and couplings is also considered, e. g. in references [9] and [10]. All these attempts address more comprehensive and general descriptions of the journal bearing operation, extending to the field of the nonlinear behaviour. Nevertheless, the "conventional" linear approach still

retains its great validity when addressing the first onset of the rotor whirl in connection with the influence of all the other properties that may improve or aggravate the tendency to instability.

The oil film instability is somewhat similar to the hysteretic instability arising from the internal friction forces, which may be considered proportional to the deformation velocities relative to a frame rotating with the shaft. As such, the rotating damping induces skew-symmetric terms in the coefficient matrix of the motion equations, which increase on increasing the angular speed, until some system eigenvalue takes a positive real part [11]. As it is assessed since a long time that the release of shrink fits and spacers is predominant in generating this effect [12], other approaches consider nonlinear models of the internal friction, which are dealt with by procedures of the Krylov-Bogoliubov type, involving solutions in terms of elliptic integrals [13]. Overall, it is found that some beneficial effect on the critical threshold is obtainable by differentiating the stiffness properties of the supports in two directions orthogonal to the shaft axis, which expedient is particularly successful when the rotor is centred at the mid-span. Owing to the resemblance of the aspects associated with the internal damping and with the oil film instability, the present analysis aims at ascertaining if the support stiffness anisotropy may produce beneficial effects for the oil film instability as well, though the two phenomena are fully different from each other. Anyhow, no damping source other than the bearing oil films will be here considered, since the main goal is just to concentrate on the combined influence of the journal bearings and the support elasticity.

2. Mathematical model

The rotor-shaft-suspension system is schematized in figure 1 and makes reference to the list of symbols reported at the end of the paper. The *z* axis of the fixed reference frame *Oxyz* refers to the non-deformed configuration of the whole system, whence the shaft axis moves away due to the rotor weight and the whirling motion (the shaft deflection is much magnified in the figure for clarity reasons). Numbers 1 to 6 refer to the displacement variables, straight arrows indicate translation along *x* and *y* and curved arrows rotation around *x* and *y*. The system is broadly assumed asymmetric with respect to the mid span, in the sense that the geometrical and mechanical properties may be different on the one and the other side of the central section, with the consequence that cylindrical and conical whirling motions are mutually coupled and must be analysed together. Nevertheless, the support elasticity is assumed symmetric but anisotropic, whence the flexibility is the same in the left and right supports, but may be different in the vertical and horizontal planes, and k_{bfx} and k_{bfy} ($\neq k_{bfx}$) denote the total stiffness between the bearings and the frame in the planes *xz* and *yz* (see figure). As the *z* axis is horizontal, the gravitational forces imply some equilibrium deflection of the shaft and some eccentricity of the journals with respect to the bearings in their contactless hydrodynamic suspension.

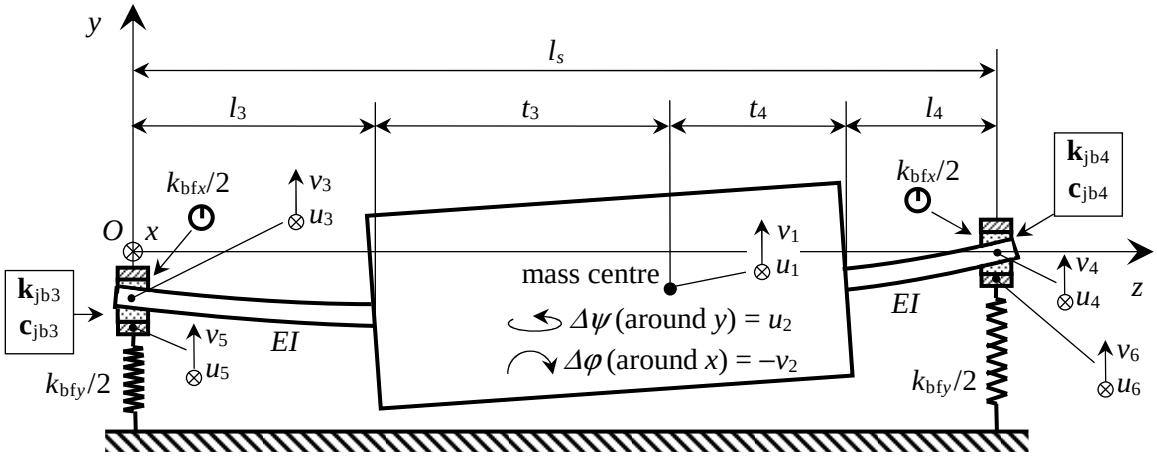

Figure 1. Scheme of asymmetric rotor on journal bearings sustained by flexible anisotropic supports. Symbols ⊗ indicate arrows entering into the plane of the figure. Symbols ⏲ indicate springs perpendicular to the plane of the figure.

All possible whirl motions arise around this equilibrium configuration.

The rotor is supposed rigid and weighty, without static or dynamic unbalance, and no mass is ascribed to the shaft and to the supports. It is assumed that the two shaft branches have the same flexural rigidity EI, where I is the areal moment of inertia of the cross section, and the Jeffcott bending stiffness $k_J = 48EI/l_s^3$ is introduced, where l_s is the distance between the bearings Indicating the rotor mass with m, the acceleration of gravity with g and the journal bearing clearance with c, the mean hydrodynamic stiffness $k_h = 0.5 \times mg/c$ is defined and used to scale all stiffness parameters. Here the weight mg is equal to the sum of the static loads F_3 and F_4 on bearings 3 and 4.

The elastic forces of the shaft are correlated through the 4×4 stiffness matrix $\mathbf{k}_s$ with the vectors $\mathbf{u}_s = \{u_1, u_2, u_3, u_4\}^T$ and $\mathbf{v}_s = \{v_1, v_2, v_3, v_4\}^T$ that collect the displacements of the rotor and the bearings, in the bending planes xz and yz respectively. Here, the symbols u_2 and v_2 represent the rotor tilt rotations around y and x, u_1 and v_1 the displacement components of the rotor centre of mass and u_3, v_3, u_4, v_4 the displacement components of the journals (see figure 1). Multiplying the stiffness matrix $\mathbf{k}_s$, by $\mathbf{u}_s$ or $\mathbf{v}_s$, one obtains the vectors of the elastic forces applied to the rotor and to the bearings. The coefficients $k_s(i,j)$ of $\mathbf{k}_s$ are calculable as the forces (or moments) required at points i to produce the unit displacement (or rotation) at points j and such that the displacements (or rotations) of all points other than j are zero. The bending flexibility of the two shaft branches is characterized by the parameters $l_3^3/(3EI)$ and $l_4^3/(3EI)$, and the shear flexibility by $l_3/(\chi GA)$ and $l_4/(\chi GA)$, where A is the area of the cross section and χ is the shear coefficient ($\chi = 0.9$ for the circular cross-section). Introducing the length ratios $L_3 = l_3/l_s$, $L_4 = l_4/l_s$, and putting

$$s_3 = \frac{k_J}{16L_3^3}\left(1 + \frac{3EI}{\chi GAl_3^2}\right)^{-1} \qquad s_4 = \frac{k_J}{16L_4^3}\left(1 + \frac{3EI}{\chi GAl_4^2}\right)^{-1} \tag{1a,b}$$

the general form of the stiffness matrix $\mathbf{k}_s$ of the shaft is

$$\mathbf{k}_s = \begin{bmatrix} s_3 + s_4 & (l_4 + t_4)s_4 - (l_3 + t_3)s_3 & -s_3 & -s_4 \\ (l_4 + t_4)s_4 - (l_3 + t_3)s_3 & (l_3 + t_3)^2 s_4 + (l_4 + t_4)^2 s_4 & (l_3 + t_3)s_3 & -(l_4 + t_4)s_4 \\ -s_3 & (l_3 + t_3)s_3 & s_3 & 0 \\ -s_4 & -(l_4 + t_4)s_4 & 0 & s_4 \end{bmatrix} \tag{2}$$

The displacements of the journal centres are different from the bearing centres, due to the eccentricity fluctuations during the time. In condition of equilibrium with no whirl, the displacements are constant and such to produce the hydrodynamic mutual forces that balance the rotor weight on the one hand and the elastic reaction forces of the supports on the other hand. Adding a whirl motion of small amplitude, the changes of the hydrodynamic forces may be regarded as linear functions of the relative displacements and velocities from the equilibrium configuration and these changes balance the corresponding changes of the elastic forces exerted by the shaft and the supports. Moreover, the changes of the elastic forces acting on the rotor balance the corresponding changes of the inertia force system of the rotor itself. Due to the system linearity, we will simply use the symbols u_i and v_i to indicate the displacements (or rotations) of the rotor, of the journals and of the bearings from the equilibrium position and will leave out the gravitational field and the static deflection. Including the supports 5 and 6 too, the two complete displacement vectors on the bending planes xz and yz are $\mathbf{u} = \{u_1, u_2, u_3, u_4, u_5, u_6\}^T$ and $\mathbf{v} = \{v_1, v_2, v_3, v_4, v_5, v_6\}^T$, where $u_2 = \Delta\psi$, $v_2 = -\Delta\varphi$, $\Delta\psi$ and $\Delta\varphi$ being the rotation around y and x, and the minus sign in the definition of v_2 permits using the same stiffness matrix $\mathbf{k}_s$ of the shaft for both bending planes, xz and yz. Hence, the total 12-dimensional displacement vector is $\mathbf{w} = \{u_1, u_2, u_3, u_4, u_5, u_6, v_1, v_2, v_3, v_4, v_5, v_6\}^T$.

It is known that any relative displacement or velocity between the journal and the bearing along either single direction, x or y, produces changes of the hydrodynamic forces in both directions x and y. Therefore, it is necessary to define one 2×2 stiffness matrix $\mathbf{k}_{jbi}$ and one 2×2 damping matrix $\mathbf{c}_{jbi}$ for each journal bearing pair, where i stands for 3 or 4. The coefficients of these matrices are usually obtained by applying small perturbations to the steady solutions of the complete Reynolds equation,

where the time-variant terms are taken into consideration as well. This process is quite complex in general and nearly always requires numerical integration throughout the lubricated region, for example by the FEM method. Moreover, the results depend on the journal bearing type, on the bearing length, on the shape of the feeding grooves and on all other characteristics.

Closed-form solutions may be obtained only for very special cases, for example the infinitely short bearing, but they may also be used for other actual arrangements with a fair approximation. Here, the coefficients for short bearings will be used as they are reported in reference [2]. They are valid for journal and bearing parallel to each other, but are acceptable as well when there is some relative slope.

Each stiffness coefficient of $\mathbf{k}_{\mathrm{jb}i}$ is given by the product of the reference stiffness $k_\mathrm{h} = 0.5\times mg/c$ and a dimensionless function of the equilibrium eccentricity ε_i, and each damping coefficient of $\mathbf{c}_{\mathrm{jb}i}$ is given by the product of k_h/ω and a dimensionless function of ε_i. These eccentricities may be different in the one and the other bearing due to the asymmetry of the loads. Minding the expression of the modified Sommerfeld number of the single bearing [1]

$$S_{\mathrm{modified},i} = \frac{\mu\omega DL}{8F_i}\left(\frac{L}{c}\right)^2 = \frac{\left(1-\varepsilon_i^2\right)^2}{\varepsilon_i\sqrt{16\varepsilon_i^2+\pi^2\left(1-\varepsilon_i^2\right)}} \qquad (i = 3 \text{ or } 4) \tag{3}$$

where μ is the oil viscosity, D and L are the bearing diameter and length, and F_i is the static load, one observes that, even for equal bearings, the static equilibrium implies that $F_3 = mg(l_4 + t_4)/l_s$ and $F_4 = mg(l_3 + t_3)/l_s$, whence $S_{\mathrm{modified},3}/S_{\mathrm{modified},4} = (l_3 + t_3)/(l_4 + t_4)$. Fixing this ratio, one of the two eccentricities, e. g. ε_4, may be calculated by trial and error as a function of the other ε_3, using equation (3). Then, putting, for $i = 3$ and 4, $H_i = [16\varepsilon_i^2 + \pi^2(1 - \varepsilon_i^2)]^{1/2}$, the matrices $\mathbf{k}_{\mathrm{jb}i}$ and $\mathbf{c}_{\mathrm{jb}i}$ may be written in the form

$$\mathbf{k}_{\mathrm{jb}i} = = k_\mathrm{h}\left(\frac{2F_i}{mg}\right)\begin{bmatrix} \frac{4}{H_i^3}[16\varepsilon_i^2+\pi^2(2-\varepsilon_i^2)] & \frac{-\pi}{\varepsilon_i H_i^3\sqrt{1-\varepsilon_i^2}}[16\varepsilon_i^4-\pi^2(1-\varepsilon_i^2)^2] \\ \frac{-\pi}{\varepsilon_i H_i^3\sqrt{1-\varepsilon_i^2}}[32\varepsilon_i^2(1+\varepsilon_i^2)+\pi^2(1-\varepsilon_i^2)(1+2\varepsilon_i^2)] & \frac{4}{H_i^3(1-\varepsilon_i^2)}[32\varepsilon_i^2(1+\varepsilon_i^2)+\pi^2(1-\varepsilon_i^2)(1+2\varepsilon_i^2)] \end{bmatrix} \tag{4a,b}$$

$$\mathbf{c}_{\mathrm{jb}i} = \frac{k_\mathrm{h}}{\omega}\left(\frac{2F_i}{mg}\right)\begin{bmatrix} \frac{2\pi\sqrt{1-\varepsilon_i^2}}{\varepsilon_i H_i^3}[\pi^2(1+2\varepsilon_i^2)-16\varepsilon_i^2] & \frac{8}{H_i^3}[16\varepsilon_i^2-\pi^2(1+2\varepsilon_i^2)] \\ \frac{8}{H_i^3}[16\varepsilon_i^2-\pi^2(1+2\varepsilon_i^2)] & \frac{2\pi}{\varepsilon_i H_i^3\sqrt{1-\varepsilon_i^2}}[48\varepsilon_i^2+\pi^2(1-\varepsilon_i^2)^2] \end{bmatrix}$$

Multiplying the matrix $\mathbf{k}_{\mathrm{jb}3}$ by the relative displacement vector, $\{u_3 - u_5,\ v_3 - v_5\}^T$, multiplying the matrix $\mathbf{c}_{\mathrm{jb}3}$ by the relative velocity vector, $\{\dot{u}_3 - \dot{u}_5, \dot{v}_3 - \dot{v}_5\}^T$, and summing, one obtains the vector of the hydrodynamic forces applied to the bearing 5. Likewise, using $\mathbf{k}_{\mathrm{jb}4}$, $\mathbf{c}_{\mathrm{jb}4}$ and the vectors $\{u_4 - u_6,\ v_4 - v_6\}^T$ and $\{\dot{u}_4 - \dot{u}_6, \dot{v}_4 - \dot{v}_6\}^T$, one gets the forces on the bearing 6. These forces balance the elastic reactions of the massless supports on the bearing 5 and 6 respectively.

The motion equations are made dimensionless defining the dimensionless counterpart $\mathbf{W}$ of the displacement vector $\mathbf{w}$ where, using the clearance c as reference deflection, the coefficients of $\mathbf{W}$ are indicated with capital letters and are given by $U_i = u_i/c$, $V_i = v_i/c$ for $i \neq 2$ (displacement), and by $U_i = u_i l_s/c$, $V_i = v_i l_s/c$ for $i = 2$ (tilt). Capital letters are used for all other dimensionless coefficients, putting $T_3 = t_3/l_s$, $T_4 = t_4/l_s$, $S_i = s_i/k_\mathrm{h}$ (i = 3,4), $K_{\mathrm{bf}x} = k_{\mathrm{bf}x}/k_\mathrm{h}$, $K_{\mathrm{bf}y} = k_{\mathrm{bf}y}/k_\mathrm{h}$, $K_{\mathrm{jb}i}(r,s) = k_{\mathrm{jb}i}(r,s)/k_\mathrm{h}$, $C_{\mathrm{jb}i}(r,s) = c_{\mathrm{jb}i}(r,s)\omega/k_\mathrm{h}$, while the dimensionless moments of inertia of the rotor are indicated by J_d (diametral) and J_a (axial), scaling the physical inertia moments by ml_s^2. The angular time variable $\theta = \omega t$ is introduced and the differentiation with respect to θ is indicated with primes, so that $d(\ldots)/dt = \omega(\ldots)'$, etc. Moreover, the reference circular frequency $\omega_0 = \sqrt{k_\mathrm{h}/m}$ and the dimensionless angular speed $\Omega = \omega/\omega_0$ are also defined.

After introducing the above dimensionless quantities, dividing the physical force equations and the physical moment equations by $k_h c$ and $k_h c l_s$, respectively, the twelve dimensionless equations of motion can be collected into the matrix form:

$$\mathbf{KW} + \mathbf{CW}' + \Omega^2\mathbf{MW}'' + \Omega^2\mathbf{GW}' = \{0\} \tag{5}$$

Here, **M** and **G** are the massive and the gyroscopic matrices, the first of which is diagonal with the coefficients (1, J_d, 0, 0, 0, 0, 1, J_d, 0, 0, 0, 0) in the diagonal, while the second has its only non-zero coefficients J_a and $-J_a$ in the positions (2,8) and (8,2) respectively. Moreover, notice that the denominator ω appearing in the expression of $\mathbf{c}_{jbi}$ cancels with the factor ω arising from the differentiation with respect to time. The total 12×12 dimensionless matrices **K** and **C** may be partitioned as follows into 6×6 matrices

$$\mathbf{K} = \begin{bmatrix} \mathbf{K}_{xx} & \mathbf{K}_{xy} \\ \mathbf{K}_{yx} & \mathbf{K}_{yy} \end{bmatrix} \qquad \mathbf{C} = \begin{bmatrix} \mathbf{C}_{xx} & \mathbf{C}_{xy} \\ \mathbf{C}_{yx} & \mathbf{C}_{yy} \end{bmatrix} \tag{6a,b}$$

Actually, let us associate the values (1,1), (2,2), (1,2), (2,1) to the indices (r,s) of the coefficients $K_{jb3}(r,s)$ and $K_{jb4}(r,s)$ in correspondence of the pairs of subscripts *xx*, *yy*, *xy*, *yx* respectively of Equations (6). Then, introducing the dummy subscripts *p* and *q*, either indicating *x* or *y*, we can write

$$\mathbf{K}_{pp} = \begin{vmatrix} S_3+S_4 & (L_4+T_4)S_4-(L_3+T_3)S_3 & -S_3 & -S_4 & 0 & 0 \\ (L_4+T_4)S_4-(L_3+T_3)S_3 & (L_3+T_3)^2S_3+(L_4+T_4)^2S_4 & (L_3+T_3)S_3 & -(L_4+T_4)S_4 & 0 & 0 \\ -S_3 & (L_3+T_3)S_3 & S_3 & 0 & 0.5K_{bfp} & 0 \\ -S_4 & -(L_4+T_4)S_4 & 0 & S_4 & 0 & 0.5K_{bfp} \\ 0 & 0 & K_{jb3}(r,s) & 0 & -K_{jb3}(r,s)-0.5K_{bfp} & 0 \\ 0 & 0 & 0 & K_{jb4}(r,s) & 0 & -K_{jb4}(r,s)-0.5K_{bfp} \end{vmatrix} \tag{7a,b}$$

$$\mathbf{K}_{pq} = \begin{vmatrix} 0 & 0 & 0 & 0 & 0 & 0 \\ 0 & 0 & 0 & 0 & 0 & 0 \\ 0 & 0 & 0 & 0 & 0 & 0 \\ 0 & 0 & 0 & 0 & 0 & 0 \\ 0 & 0 & K_{jb3}(r,s) & 0 & -K_{jb3}(r,s) & 0 \\ 0 & 0 & 0 & K_{jb4}(r,s) & 0 & -K_{jb4}(r,s) \end{vmatrix}$$

Moreover, $\mathbf{C}_{pp}$ and $\mathbf{C}_{pq}$ have null coefficients in the first four rows and their fifth and sixth rows are similar to $\mathbf{K}_{pp}$ and $\mathbf{K}_{pq}$, save that all coefficients K_{jb3or4} are replaced by C_{jb3or4} and K_{bfp} does no longer appear.

If the rotor-shaft-bearing system is symmetric with respect to the mid-span, one has $L_3 + T_3 = L_4 + T_4 = 0.5$, $S_3 = S_4 = S$, $K_{jb3}(r,s) = K_{jb4}(r,s) = K_{jb}(r,s)$, $C_{jb3}(r,s) = C_{jb4}(r,s) = C_{jb}(r,s)$, and the differential system (5) splits into two subsystems of 6 equations in 6 unknowns. One system refers to the cylindrical motions and the other to the conical motions, which are indeed uncoupled in the symmetric case. Actually, considering the twelve equations contained in the matrix equation (5), summing the third and fourth equations, summing the fifth and sixth equations, summing the ninth and tenth equations, summing the eleventh and twelfth equations, associating these sums to the first and seventh equations and introducing the translational displacements $U_{tj} = (U_3 + U_4)/2$, $V_{tj} = (V_3 + V_4)/2$, $U_{tb} = (U_5 + U_6)/2$, $V_{tb} = (V_5 + V_6)/2$ of the journals and the bearings, the sixth order differential system for the six cylindrical unknowns, U_1, U_{tj}, U_{tb}, V_1, V_{tj}, V_{tb}, is

$$
\begin{aligned}
&\Omega^2 U''_1 + 2S\left(U_1 - U_{\mathrm{tj}}\right) = 0\\
&K_{\mathrm{bf}x} U_{\mathrm{tb}} - 2S\left(U_1 - U_{\mathrm{tj}}\right) = 0\\
&K_{\mathrm{jb}}(1,1)\left(U_{\mathrm{tj}} - U_{\mathrm{tb}}\right) + C_{\mathrm{jb}}(1,1)\left(U'_{\mathrm{tj}} - U'_{\mathrm{tb}}\right) + K_{\mathrm{jb}}(1,2)\left(V_{\mathrm{tj}} - V_{\mathrm{tb}}\right) + C_{\mathrm{jb}}(1,2)\left(V'_{\mathrm{tj}} - V'_{\mathrm{tb}}\right) - \frac{K_{\mathrm{bf}x}}{2} U_{\mathrm{tb}} = 0\\
&\Omega^2 V''_1 + 2S\left(V_1 - V_{\mathrm{tj}}\right) = 0\\
&K_{\mathrm{bf}y} V_{\mathrm{tb}} - 2S\left(V_1 - V_{\mathrm{tj}}\right) = 0\\
&K_{\mathrm{jb}}(2,1)\left(U_{\mathrm{tj}} - U_{\mathrm{tb}}\right) + C_{\mathrm{jb}}(2,1)\left(U'_{\mathrm{tj}} - U'_{\mathrm{tb}}\right) + K_{\mathrm{jb}}(2,2)\left(V_{\mathrm{tj}} - V_{\mathrm{tb}}\right) + C_{\mathrm{jb}}(2,2)\left(V'_{\mathrm{tj}} - V'_{\mathrm{tb}}\right) - \frac{K_{\mathrm{bf}y}}{2} V_{\mathrm{tb}} = 0
\end{aligned}
\tag{8}
$$

Then, subtracting the third from the fourth equation, subtracting the fifth from the sixth equation, subtracting the ninth from the tenth equation, subtracting the eleventh from the twelfth equation, associating these difference to the second and eighth equations and introducing the rotations $U_{\mathrm{rj}} = (U_4 - U_3)/2$, $V_{\mathrm{rj}} = (V_4 - V_3)/2$, $U_{\mathrm{rb}} = (U_6 - U_5)/2$, $V_{\mathrm{rb}} = (V_6 - V_5)/2$ of the lines connecting the journal and bearing, the sixth order system for the six conical unknowns, U_2, U_{rj}, U_{rb}, V_2, V_{rj}, V_{rb}, is

$$
\begin{aligned}
&J_{\mathrm{d}}\Omega^2 U''_2 + J_{\mathrm{a}}\Omega^2 V'_2 + \frac{S}{2} U_2 - S U_{\mathrm{rj}} = 0\\
&K_{\mathrm{bf}x} U_{\mathrm{rb}} - S U_2 + 2S U_{\mathrm{rj}} = 0\\
&K_{\mathrm{jb}}(1,1)\left(U_{\mathrm{rj}} - U_{\mathrm{rb}}\right) + C_{\mathrm{jb}}(1,1)\left(U'_{\mathrm{rj}} - U'_{\mathrm{rb}}\right) + K_{\mathrm{jb}}(1,2)\left(V_{\mathrm{rj}} - V_{\mathrm{rb}}\right) + C_{\mathrm{jb}}(1,2)\left(V'_{\mathrm{rj}} - V'_{\mathrm{rb}}\right) - \frac{K_{\mathrm{bf}x}}{2} U_{\mathrm{rb}} = 0\\
&J_{\mathrm{d}}\Omega^2 V''_2 - J_{\mathrm{a}}\Omega^2 U'_2 + \frac{S}{2} V_2 - S V_{\mathrm{rj}} = 0\\
&K_{\mathrm{bf}y} V_{\mathrm{rb}} - S V_2 + 2S V_{\mathrm{rj}} = 0\\
&K_{\mathrm{jb}}(2,1)\left(U_{\mathrm{rj}} - U_{\mathrm{rb}}\right) + C_{\mathrm{jb}}(2,1)\left(U'_{\mathrm{rj}} - U'_{\mathrm{rb}}\right) + K_{\mathrm{jb}}(2,2)\left(V_{\mathrm{rj}} - V_{\mathrm{rb}}\right) + C_{\mathrm{jb}}(2,2)\left(V'_{\mathrm{rj}} - V'_{\mathrm{rb}}\right) - \frac{K_{\mathrm{bf}y}}{2} V_{\mathrm{rb}} = 0
\end{aligned}
\tag{9}
$$

If the shaft is perfectly rigid (i. e. if $k_{\mathrm{J}} \to \infty$), the coefficients $S_i = s_i/k_{\mathrm{h}}$ of the stiffness matrix (7a) diverge by equations (1), but should we divide the differential system (5) by k_{J}, the first, second, seventh and eight equations would reduce to the only terms containing the coefficients S_i/k_{J} of the stiffness matrix $\mathbf{K}_{pp}$ (7a) and would permit solving for U_1 and U_2 as two functions of U_3 and U_4, and for V_1 and V_2 as two functions of V_3 and V_4. Proceeding like that, we get in practice the result that the displacements of the centres of the rotor and the bearings conform to the laws of rigid motion and may eliminate the four state variables U_1, U_2, V_1 and V_2. Actually, minding that $L_3 + T_3 + L_4 + T_4 = 1$, we have

$$
\begin{aligned}
U_1 &= (L_4 + T_4)U_3 + (L_3 + T_3)U_4 \qquad U_2 = U_4 - U_3\\
V_1 &= (L_4 + T_4)V_3 + (L_3 + T_3)V_4 \qquad V_2 = V_4 - V_3
\end{aligned}
\tag{10a,b,c,d}
$$

and replacing these expressions into equations (3-7), it is observable that, though the dimensionless stiffness coefficients S_3 and S_4 of the shaft diverge, the sums of the corresponding terms appear in the indeterminate form $0 \times \infty$ in the differential system (5). Nevertheless, summing the first, third and fourth of equations (5), and then summing the seventh, ninth and tenth equations, the indeterminate terms cancel each other and one obtains the translational equilibrium equations of the whole rotor-bearing system. Likewise, subtracting the third equation multiplied by L_3+T_3 from the second one, then summing the fourth one multiplied by L_4+T_4, and proceeding like that with the seventh, ninth and tenth

equations, one obtains the rotational equilibrium equations. The fifth, sixth, eleventh and twelfth equations of the system (5) remain unchanged. Summing up, we have now arrive at a reduced differential system of 8 equations in the 8 state variables $\{U_3, U_4, U_5, U_6, V_3, V_4, V_5, V_6\}$:

$$
\begin{aligned}
&\Omega^2[(L_4+T_4)U"_3+(L_3+T_3)U"_4]+0.5K_{\mathrm{bf}x}(U_5+U_6)=0\\
&\Omega^2J_{\mathrm{d}}(U"_4-U"_3)+\Omega^2J_{\mathrm{a}}(V'_4-V'_3)+0.5K_{\mathrm{bf}x}[(L_4+T_4)U_6-(L_3+T_3)U_5]=0\\
&K_{\mathrm{jb3}}(1,1)(U_3-U_5)+C_{\mathrm{jb3}}(1,1)(U'_3-U'_5)+K_{\mathrm{jb3}}(1,2)(V_3-V_5)+C_{\mathrm{jb3}}(1,2)(V'_3-V'_5)\\
&\qquad\qquad -0.5K_{\mathrm{bf}x}U_5=0\\
&K_{\mathrm{jb4}}(1,1)(U_4-U_6)+C_{\mathrm{jb4}}(1,1)(U'_4-U'_6)+K_{\mathrm{jb4}}(1,2)(V_4-V_6)+C_{\mathrm{jb4}}(1,2)(V'_4-V'_6)\\
&\qquad\qquad -0.5K_{\mathrm{bf}x}U_6=0\\
&\Omega^2[(L_4+T_4)V"_3+(L_3+T_3)V"_4]+0.5K_{\mathrm{bf}y}(V_5+V_6)=0\\
&\Omega^2J_{\mathrm{d}}(V"_4-V"_3)-\Omega^2J_{\mathrm{a}}(U'_4-U'_3)+0.5K_{\mathrm{bf}y}[(L_4+T_4)V_6-(L_3+T_3)V_5]=0\\
&K_{\mathrm{jb3}}(2,1)(U_3-U_5)+C_{\mathrm{jb3}}(2,1)(U'_3-U'_5)+K_{\mathrm{jb3}}(2,2)(V_3-V_5)+C_{\mathrm{jb3}}(2,2)(V'_3-V'_5)\\
&\qquad\qquad -0.5K_{\mathrm{bf}y}V_5=0\\
&K_{\mathrm{jb4}}(2,1)(U_4-U_6)+C_{\mathrm{jb4}}(2,1)(U'_4-U'_6)+K_{\mathrm{jb4}}(2,2)(V_4-V_6)+C_{\mathrm{jb4}}(2,2)(V'_4-V'_6)\\
&\qquad\qquad -0.5K_{\mathrm{bf}y}V_6=0
\end{aligned}
\tag{11}
$$

In the further hypothesis that the rotor-shaft-bearing system is symmetric with respect to the mid-span, the differential system (11) splits into two subsystems of 4 equations in 4 unknowns, which describe the cylindrical and conical motions. Summing the third and fourth of equations (11), summing the seventh and eighth equations, associating these sums to the first and fifth equations respectively, minding equations (10a) and (10c) and putting $U_{\mathrm{t}} = (U_5 + U_6)/2$, $V_{\mathrm{t}} = (V_5 + V_6)/2$, the sixth order cylindrical system is

$$
\begin{aligned}
&\Omega^2U"_1+K_{\mathrm{bf}x}U_{\mathrm{t}}=0\\
&K_{\mathrm{jb}}(1,1)(U_1-U_{\mathrm{t}})+C_{\mathrm{jb}}(1,1)(U'_1-U'_{\mathrm{t}})+K_{\mathrm{jb}}(1,2)(V_1-V_{\mathrm{t}})+C_{\mathrm{jb}}(1,2)(V'_1-V'_{\mathrm{t}})-0.5K_{\mathrm{bf}x}U_{\mathrm{t}}=0\\
&\Omega^2V"_1+K_{\mathrm{bf}y}V_{\mathrm{t}}=0\\
&K_{\mathrm{jb}}(2,1)(U_1-U_{\mathrm{t}})+C_{\mathrm{jb}}(2,1)(U'_1-U'_{\mathrm{t}})+K_{\mathrm{jb}}(2,2)(V_1-V_{\mathrm{t}})+C_{\mathrm{jb}}(2,2)(V'_1-V'_{\mathrm{t}})-0.5K_{\mathrm{bf}y}V_{\mathrm{t}}=0
\end{aligned}
\tag{12}
$$

Subtracting the third from the fourth of equations (11), subtracting the seventh from the eighth equation, associating these difference to the second and sixth equations respectively, minding equations (10b) and (10d) and putting $U_{\mathrm{r}} = U_6 - U_5$, $V_{\mathrm{r}} = V_6 - V_5$, the sixth order conical system is

$$
\begin{aligned}
&\Omega^2J_{\mathrm{d}}U"_2+\Omega^2J_{\mathrm{a}}V'_2+0.25K_{\mathrm{bf}x}U_{\mathrm{r}}=0\\
&K_{\mathrm{jb}}(1,1)(U_2-U_{\mathrm{r}})+C_{\mathrm{jb}}(1,1)(U'_2-U'_{\mathrm{r}})+K_{\mathrm{jb}}(1,2)(V_2-V_{\mathrm{r}})+C_{\mathrm{jb}}(1,2)(V'_2-V'_{\mathrm{r}})-0.5K_{\mathrm{bf}x}U_{\mathrm{r}}=0\\
&\Omega^2J_{\mathrm{d}}V"_2-\Omega^2J_{\mathrm{a}}U'_2+0.25K_{\mathrm{bf}y}V_{\mathrm{r}}=0\\
&K_{\mathrm{jb}}(2,1)(U_2-U_{\mathrm{r}})+C_{\mathrm{jb}}(2,1)(U'_2-U'_{\mathrm{r}})+K_{\mathrm{jb}}(2,2)(V_2-V_{\mathrm{r}})+C_{\mathrm{jb}}(2,2)(V'_2-V'_{\mathrm{r}})-0.5K_{\mathrm{bf}y}V_{\mathrm{r}}=0
\end{aligned}
\tag{13}
$$

Notice that in the case of uncoupling, the cylindrical modes are symmetric and the conical ones are anti symmetric, because the characteristic roots of each motion type are not such for the other type, involving the trivial solution for the latter.

3. Results

The dynamical behaviour of a rigid and symmetric rotor-shaft set is described by the differential systems (12) and (13), for the cylindrical and conical motions respectively. The latter ones are more stable in general, as they mostly grow up above higher threshold speeds of the rotor, so that the

cylindrical motions define the limits of the stable running range for most bearing eccentricities and our focus will be here on these motions mainly. The order of the differential system (12) is just six and the stability analysis is simple for this case, where closed-form solutions are attainable for the eigenvalue problem. Yet, these simple results elucidate quite well the effects of the support anisotropy on the stability of the machine and provide realistic clues about the conduct of more complex systems.

Assume solutions of the type $\exp(\Lambda\theta/\Omega)$ where Λ is a dimensionless characteristic number, obtained by scaling the actual eigenvalue λ of the time domain by ω_0, so that $\Lambda\theta/\Omega = \lambda t$. Replacing these solutions into system (12), a sixth-degree characteristic equation in Λ may be extracted, whose roots must have negative real parts for stability. Therefore, the instability thresholds correspond to pairs of pure imaginary roots, $\Lambda = \pm \mathrm{i}\Gamma$, which may be calculated, as functions of the angular speed Ω, by separately cancelling the real and imaginary parts of the characteristic equation. Putting $K_{kc} = K_{\mathrm{jb}}(1,1)C_{\mathrm{jb}}(2,2) + K_{\mathrm{jb}}(2,2)C_{\mathrm{jb}}(1,1) - K_{\mathrm{jb}}(1,2)C_{\mathrm{jb}}(2,1) - K_{\mathrm{jb}}(2,1)C_{\mathrm{jb}}(1,2)$ for brevity, we get

$$K_{\mathrm{bf}x}K_{\mathrm{bf}y}\Gamma^4 - 2\left[K_{\mathrm{bf}x}K_{\mathrm{jb}}(2,2)\left(K_{\mathrm{bf}y} - \Gamma^2\right) + K_{\mathrm{bf}y}K_{\mathrm{jb}}(1,1)\left(K_{\mathrm{bf}x} - \Gamma^2\right)\right]\Gamma^2 + 4\left(K_{\mathrm{bf}x} - \Gamma^2\right)\left(K_{\mathrm{bf}y} - \Gamma^2\right)\left[\det\left(K_{\mathrm{jb}}\right) - \frac{\Gamma^2}{\Omega^2}\det\left(C_{\mathrm{jb}}\right)\right] = 0 \qquad \text{(real)} \tag{14a,b}$$

$$\left\{\left(2K_{kc} + K_{\mathrm{bf}x}C_{\mathrm{jb}}(2,2) + K_{\mathrm{bf}y}C_{\mathrm{jb}}(1,1)\right)\Gamma^4 - \left[2K_{kc}\left(K_{\mathrm{bf}x} + K_{\mathrm{bf}y}\right) + K_{\mathrm{bf}x}K_{\mathrm{bf}y}\left(C_{\mathrm{jb}}(1,1) + C_{\mathrm{jb}}(2,2)\right)\right]\Gamma^2 + 2K_{kc}K_{\mathrm{bf}x}K_{\mathrm{bf}y}\right\}\left(\pm\frac{2\mathrm{i}\Gamma}{\Omega}\right) = 0 \qquad \text{(imaginary)}$$

Varying the journal bearing eccentricity ε from 0 to 1, the coefficients of the matrices $\mathbf{K}_{\mathrm{jb}}$ and $\mathbf{C}_{\mathrm{jb}}$ may be calculated, e. g. using equations (4) for the short bearing case, otherwise by numerical integration of the perturbed Reynolds equation, and then, omitting the non-zero factor ($\pm 2\mathrm{i}\Gamma/\Omega$), equation (14b) yields two solutions, Γ_1^2 and Γ_2^2, which are acceptable if positive. Replacing the one and the other solution into Equation (14a), it is possible to solve for Ω^2, thus obtaining two values of the angular speed, the lowest of which gives the actual instability threshold. Hence, it is possible to trace a stability map on the plane (Ω, ε) and report on this map also the frequencies Γ of the incipient whirling motions.

As may be expected, the shapes of the instability curves change continuously on varying the stiffness parameters of the supports, $K_{\mathrm{bf}x}$ and $K_{\mathrm{bf}y}$. Yet, one of these parameters may be held fixed, e. g. the stiffness $K_{\mathrm{bf}x}$ in the horizontal plane, for which a rather large value is advisable in order that the supports are not too much loose, whereas the other, $K_{\mathrm{bf}y}$, may be varied. In practice, it is possible to bring into focus only two extreme cases: $K_{\mathrm{bf}y} = K_{\mathrm{bf}x}$ (tight isotropic stiffness) and $K_{\mathrm{bf}y} = K_{\mathrm{bf}y,\mathrm{minimum}}$ (flexible supports in the vertical plane). The shapes of the diagrams for the intermediate configurations may be guessed somehow by supposing to deform either of the two extreme plots continuously towards the other, as described below.

Figure 2 a,b shows the stability maps for a rigid and symmetric rotor-shaft system held up by more or less flexible supports. The critical curves are traced in this and in the following figures as functions of the common journal eccentricity ε for symmetric systems, or else of ε_3 in the case of asymmetry, whose ranges are between 0 and 1. This choice permits giving a general description of the system behaviour, released from the values of the other bearing parameters, such as the viscosity, the length, etc., which would be specifically involved expressing the results as functions e. g. of the load. Realistic values were ascribed to the geometrical and physical parameters, as reported in the captions. The ratios r/l_s and $(t_3 + t_4)/l_s$ were assigned to specify the main sizes of the rotor and calculate the dimensionless moments of inertia, making the assumption of an ideal cylindrical shape, so that $J_{\mathrm{a}} = (r/l_s)^2/2$ and $J_{\mathrm{d}} = (r/l_s)^2/4 + (t_3 + t_4)^2/(12l_s^2)$. The diagrams refer to two distinct values of the vertical stiffness $K_{\mathrm{bf}y}$ and contain also the threshold curve of the isotropic stiff case for a comparison purpose.

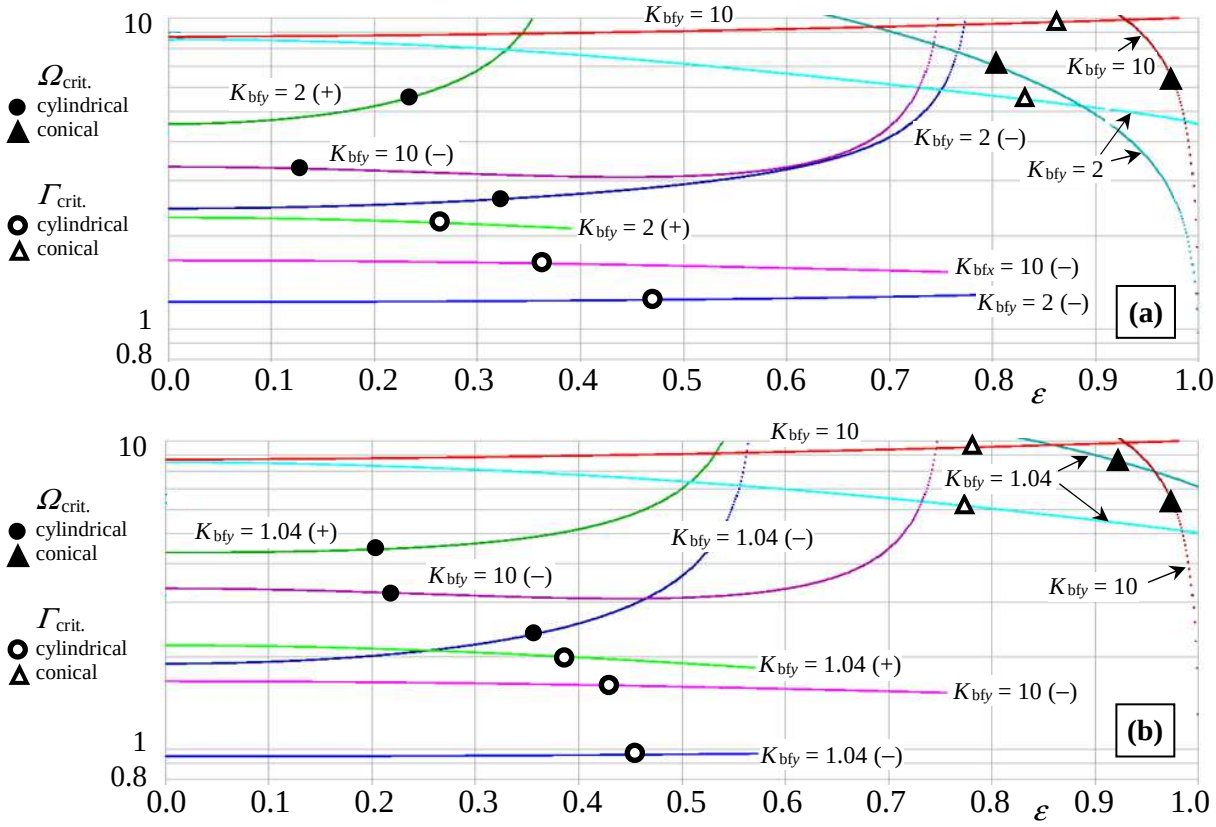

Figure 2 a,b. Dimensionless critical speed $\Omega_{\text{crit.}}$ and frequency $\Gamma_{\text{crit.}}$, vs. bearing eccentricity ε for a rigid symmetric rotor-shaft system. Data: $r/l_s = 0.125$, $(t_3+t_4)/l_s = 0.5$, $l_i = t_i$, $K_{bfx} = 10$, $\varepsilon_4 = \varepsilon_3 = \varepsilon$

a) Comparison between different vertical stiffness of supports: $K_{bfy} = 2$ and $K_{bfy} = 10$ (= K_{bfx})

b) Comparison between different vertical stiffness of supports: $K_{bfy} = 1.04$ and $K_{bfy} = 10$ (= K_{bfx})

Signs + and – in the brackets refer to the two roots of equation (14b) (± square root of discriminant).

For $K_{bfy} = K_{bfx} = K_{bf}$ (isotropic stiff case) equation (14b) reduces to

$$(K_{\text{bf}} - \Gamma^2)\left[2K_{kc}(K_{\text{bf}} - \Gamma^2) - K_{\text{bf}}\Gamma^2\left(C_{\text{jb}}(1,1) + C_{\text{jb}}(2,2)\right)\right] = 0 \qquad \text{whose roots are}$$

$$\Gamma^2 = \frac{2K_{kc}K_{\text{bf}}}{2K_{kc} + K_{\text{bf}}\left(C_{\text{jb}}(1,1) + C_{\text{jb}}(2,2)\right)} \qquad \text{and} \qquad \Gamma^2 = K_{\text{bf}} \tag{15a,b,c}$$

These two roots may be found to correspond to the minus sign (15b) and plus sign (15c) in front of the square root of the discriminant in the solution formula of the quadratic equation (14b).

On the other hand, equation (14a) reduces to

$$\frac{\Gamma^2}{\Omega^2} = \frac{1}{\det(C_{\text{jb}})}\left[\det(K_{\text{jb}}) + \frac{\Gamma^4 K_{\text{bf}}^2}{4(K_{\text{bf}} - \Gamma^2)^2} - \frac{\Gamma^2 K_{\text{bf}}}{2(K_{\text{bf}} - \Gamma^2)}\left(K_{\text{jb}}(1,1) + K_{\text{jb}}(2,2)\right)\right] \tag{16}$$

and replacing the second root (15c), one sees that the ratio Γ/Ω diverges. Replacing the first root (15b) on the contrary, Γ/Ω is finite and one may calculate the critical angular speed Ω.

Letting $K_{\text{bf}} \to \infty$, the second root (15c) diverges, whereas the first one (15b) tends to $2K_{kc}/[C_{\text{jb}}(1,1) + C_{\text{jb}}(2,2)]$, whence equation (16) leads to

$$\Omega^2 \to \frac{2\det\left(C_{\mathrm{jb}}\right)}{\left[\frac{\left(C_{\mathrm{jb}}(1,1)+C_{\mathrm{jb}}(2,2)\right)\det\left(K_{\mathrm{jb}}\right)}{K_{kc}}+\frac{K_{kc}}{\left(C_{\mathrm{jb}}(1,1)+C_{\mathrm{jb}}(2,2)\right)}-\left(K_{\mathrm{jb}}(1,1)+K_{\mathrm{jb}}(2,2)\right)\right]} \tag{17}$$

Figures 2 a and b show the results by equations (14-17) depending on the common eccentricity ε of the journals and point out that, for $K_{\mathrm{bfy}} = K_{\mathrm{bfx}} = K_{\mathrm{bf}}$ and large values of K_{bf} (= 10 in Figure 2), the critical speed Ω diverges when ε is close to 0.75. Actually, a vertical asymptote appears for each critical curve of all other cases, either with isotropic or anisotropic support stiffness, and its position may be located equating to zero the ratio Γ^2/Ω^2 in equation (14a), eliminating then Γ^2 between equations (14a) and (14b) and solving the resulting equation for ε by some trial and error procedure.

Imagining to decrease the vertical stiffness K_{bfy} from the maximum value, which is assumed equal to K_{bfx}, towards the value of maximum flexibility $K_{\mathrm{bfy,minimum}}$, the two curves of the critical angular speed corresponding to the roots with the plus and minus signs of the quadratic equation (14b) might be seen changing their shape gradually and while the former might be seen descending and moving towards the higher eccentricities (plus sign), the latter might be seen moving towards the lower eccentricities (minus sign). In practice, the optimal vertical flexibility of the supports, say $1/K_{\mathrm{bfy,minimum}}$, could be chosen when their vertical asymptotes nearly come to coincide. This trend is visible comparing figure 2a (intermediate flexibility) with 2b (maximum flexibility). The former does not offer benefits in comparison with the stiff supports (compare the plots $K_{\mathrm{bfy}} = 10$ (–) and $K_{\mathrm{bfy}} = 2$ (–) for $\Omega_{\mathrm{crit.}}$), whereas the latter appears convenient when operating in the range of the largest eccentricities, that is for large loads and low rotational speeds (compare the plots $K_{\mathrm{bfy}} = 10$ (–) and $K_{\mathrm{bfy}} = 1.04$ (–) for $\Omega_{\mathrm{crit.}}$). This behaviour may be conveniently exploited by loosening the support vertical stiffness a little for large loads and low speeds, and tightening it in the complementary range of the low loads and large speeds. The critical speeds associated with the conical motions show up only for very high eccentricities, which are undesirable however due to the danger of possible contacts between the journal and the bearing.

The typical trend of the critical curves of the rigid-symmetric rotor-shaft system recurs in practice without conceptual differences for all other more complex cases, where for example the shaft is flexible and the rotor is not centred. Yet, the full differential system (5) of the twelfth order must now be used, inserting the matrices (6) and (7), and the solution must be searched by numerical procedures.

Putting the solution of equation (5) in the form $\mathbf{W} = \mathbf{W}_0\exp(\Lambda\theta/\Omega)$, the characteristic determinant yields a 12th degree algebraic equation: $E(\Lambda) = b_0\Lambda^{12} + b_1\Lambda^{11} + \ldots + b_{11}\Lambda + b_{12} = 0$. The constant term is given by $b_{12} = \det(\mathbf{K})$, while the other coefficients b_i may be calculated by a sort of "collocation" method, choosing six distinct numbers n, e. g. $n = 1, 2, 3, 4, 5, 6$, and writing

$$\begin{aligned} b_0 n^{12} + b_1 n^{11} + \ldots + b_{10} n^2 + b_{11} n &= -\det(\mathbf{K}) + E(n) \\ b_0 n^{12} - b_1 n^{11} + \ldots + b_{10} n^2 - b_{11} n &= -\det(\mathbf{K}) + E(-n) \end{aligned} \tag{18a,b}$$

Summing and subtracting the 6 equations (18a) and the 6 equations (18b), one gets two 6×6 algebraic systems, for the even and odd coefficients separately, and the computational time for calculating the b_i is thus much reduced comparing with the complete 12×12 system:

$$b_0 n^{12} + b_2 n^{10} + \ldots + b_{10} n^2 = -\det(\mathbf{K}) + \frac{E(n)+E(-n)}{2} \qquad b_1 n^{11} + b_3 n^9 + \ldots + b_{11} n = \frac{E(n)-E(-n)}{2} \tag{19a,b}$$

where the right hands are to be considered as known quantities because the determinants $E(n)$ and $E(-n)$ are easily calculable by common numerical routines.

For each value of ε, the stability may be checked starting from a tentative critical speed Ω, increasing it by steps, calculating the coefficients of the characteristic polynomial by means of the described procedure and applying the Routh method until an eigenvalue with positive real part is

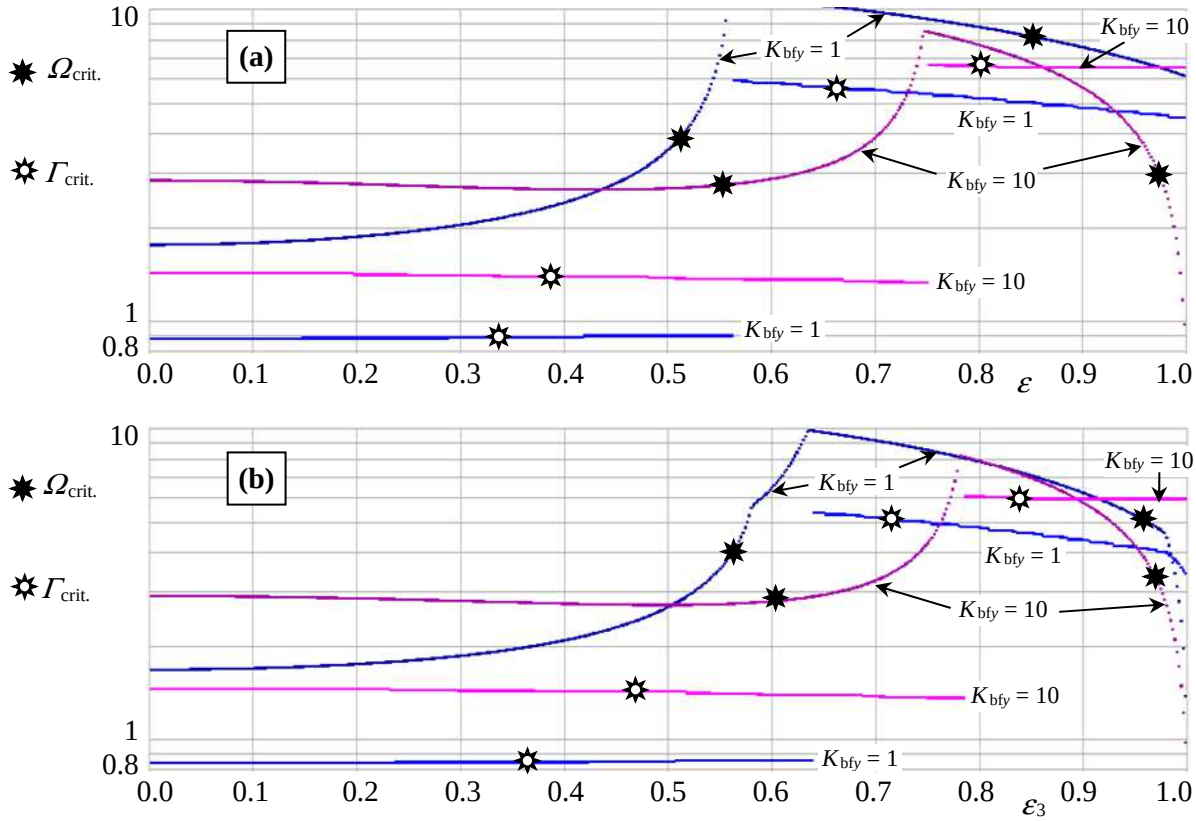

Figure 3 a,b. Dimensionless critical speed $\Omega_{crit.}$ and frequency $\Gamma_{crit.}$ vs. bearing eccentricity ε_3. Case of flexible shaft and symmetry or asymmetry of the system. Cylindrical and conical motions are detected together. Data: $r/l_s = 0.125$, $(t_3+t_4)/l_s = 0.5$, $l_i = t_i$, $k_J/k_h = 1$, $K_{bfx} = 10$, $3EI/(\chi GAl_s^2) = 0.005$

a) Symmetric system: $(l_3+t_3)/l_s = 0.5$, $(l_4+t_4)/l_s = 0.5$, $\varepsilon_4 = \varepsilon_3 = \varepsilon$

b) Asymmetric system: $(l_3+t_3)/l_s = 0.3$, $(l_4+t_4)/l_s = 0.7$, $\varepsilon_4 = \varepsilon_4(\varepsilon_3) \neq \varepsilon_3$ by equation (3).

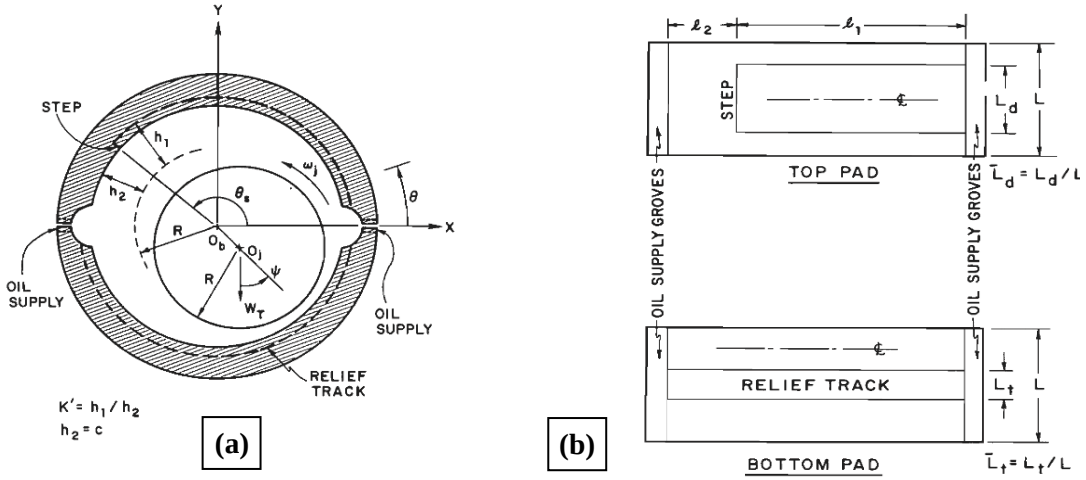

Figure 4 a,b. Step journal bearing: a) cross-section, b) top and bottom pads (from [14]). Case study: $L/D = 1$ $h_1/c = 3$ $L_d/L = 0.75$ $L_t/L = 0.25$ $\theta_s = 125°$ $\mathrm{Re} = \rho\omega rc/\mu = 210$

found. Then, after fixing the pair (ε, Ω), the variable Λ is replaced by $\pm i\Gamma$ in $E(\Lambda)$ and Γ is varied as well by trial and error until the real and imaginary parts of $E(\pm i\Gamma)$ approach zero together with

sufficient accuracy. Thus, also the critical frequencies are obtained.

The general approach permits studying the stability conduct of asymmetric system, where the Sommerfeld numbers of the two bearings are proportional to their distances from the mass centre of the rotor, as previously said, and the matrices $\mathbf{K}_{jbi}$ are different. Yet, the results appear similar to the symmetric rigid rotor analysed before, with the same favourable effect of the vertical compliance of the supports in the range of large eccentricities and of the stiff supports for low eccentricity.

Figures 3 a and b report the threshold curves for the general case of a flexible shaft, in the symmetric and asymmetric configurations, where the said properties are clearly shown, though the differences may appear softened due to logarithmic scale. It is interesting that the influence of the anisotropy is negligibly affected by the increase of the asymmetry, differently from the stabilization of the hysteretic shafts, where it decays remarkably on increasing the asymmetry [13]. The results of figure 3 a for the symmetric case agree exactly with those obtainable by applying the same procedure separately to the 6th degree characteristic equations of the uncoupled differential systems (8) and (9). Moreover, imposing a very large value to the ratio k_J/k_h, to simulate a rigid shaft, critical curves are obtainable that are identical to figure 2.

Apart from the two-mode operation, realized by tightening and loosening the vertical stiffness for the low and high eccentricities respectively, another strategy could consist in using soft vertical

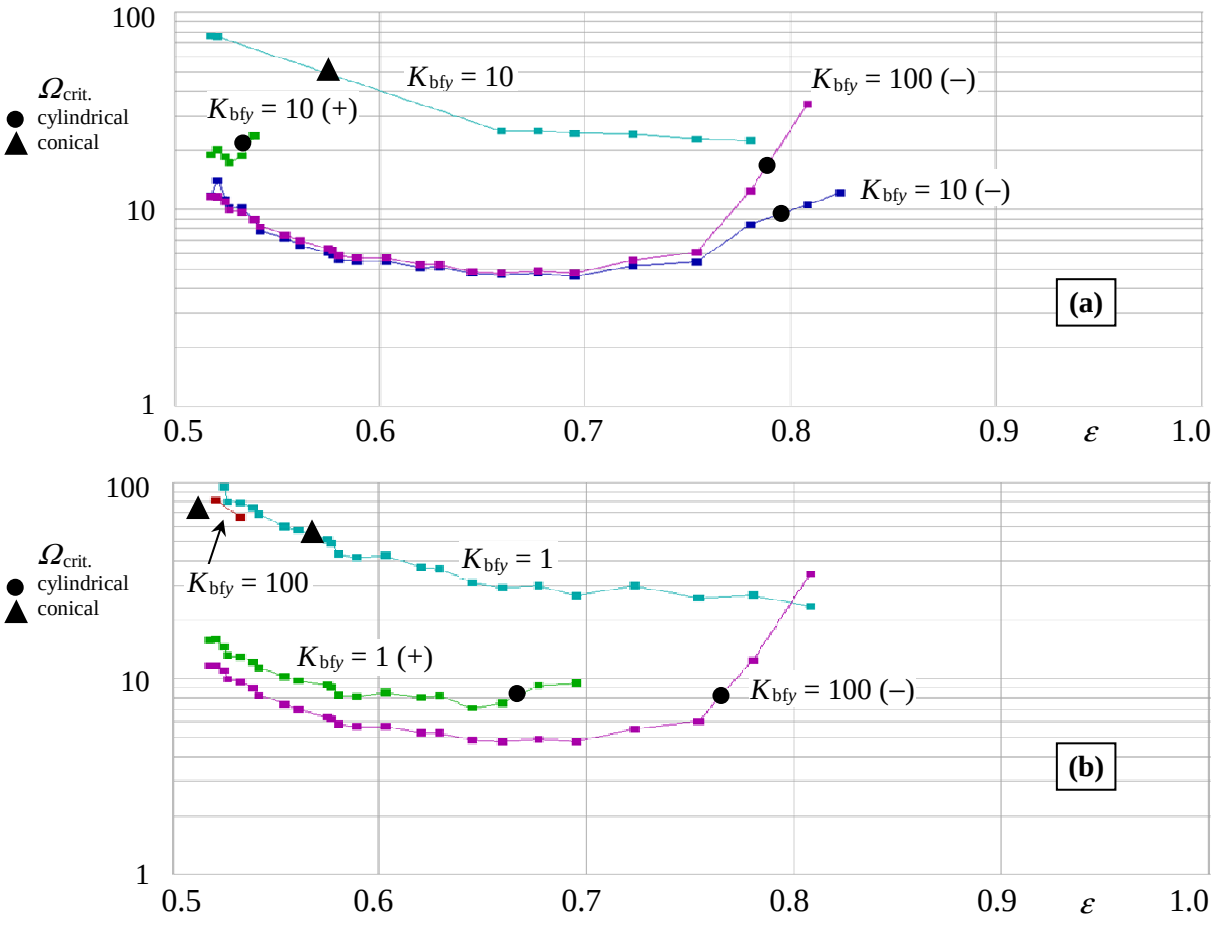

Figure 5 a,b. Dimensionless critical speed vs. bearing eccentricity for a rigid and symmetric rotor-shaft system. Data: $r/l_s = 0.125$, $(t_3+t_4)/l_s = 0.5$, $l_i = t_i$, $K_{bfx} = 100$, $\varepsilon_4 = \varepsilon_3 = \varepsilon$

a) Comparison between different vertical stiffness of supports: $K_{bfy} = 10$ and $K_{bfy} = 100$ (= K_{bfx})

b) Comparison between different vertical stiffness of supports: $K_{bfy} = 1$ and $K_{bfy} = 100$ (= K_{bfx})

Signs + and – inside brackets refer to the two roots of equation (14b) (± square root of discriminant).

stiffness and journal bearing arrangements exhibiting a better response than the plain bearings for low eccentricities, in order to combine the advantages of the two solutions. For example figure 4, taken from reference [14], shows the scheme of a step journal bearing, also called pressure-dam bearing, where the step of the top pad produces a stabilizing load increase when the bearing speed increases.

Here, this bearing type is combined with the differential stiffness of the supports. The advantages achievable can be observed in the figures 5 a and b, which were obtained similarly to the plain bearing case, but replacing the matrices of equations (4a,b) with the stiffness and damping coefficients taken from the numerical results of figures 5, 8 and 9 of [14]. Fixing a large stiffness level of the supports in the horizontal plane and supposing to decrease the vertical stiffness gradually from that level, the trend of the threshold curves is similar to the plain bearing case, but a remarkable growth of the anisotropic critical speed is observable on decreasing the eccentricity.

4. Conclusions

1) Lubricated journal bearings are widely used in rotating machine, but the carrying capacity of the oil film joins up with possible instability conditions on increasing the rotational speed. From the mathematical point of view, this trend is associated with the asymmetry of the stiffness matrix of the journal bearings.
2) Some advantages may be obtained by differentiating the support stiffness in the horizontal and vertical planes. The results indicate appreciable benefits in the range of large eccentricities (low speeds and large loads), whereas the instability thresholds worsen a little for large speeds and low loads.
3) The drawback mentioned in the previous point 2 may be remedied by conceiving a two-mode operation, where the supports are tight in both the horizontal and vertical directions for low bearing eccentricities, and somewhat loosened in the vertical direction for high eccentricities.
4) Otherwise, it is possible to combine the favourable properties of step journal bearings for low eccentricities with the differential stiffness of the support and avoid the two-mode working.

List of symbols

b_i	dimensionless coefficients of characteristic equation $E(\Lambda) = 0$ (i = 0, 1, 2, …, 12)
c	journal bearing clearance [m]
$\mathbf{c}_{jbi}$ \ $\mathbf{c}_{jb}$	physical damping matrix of journal bearing (i = 3 or 4) \ symmetric case [Ns/m]
$\mathbf{C}$	total dimensionless damping matrix
$\mathbf{C}_{jbi} = \omega\mathbf{c}_{jbi}/k_h$ \ $\mathbf{C}_{jb}$	dimensionless damping matrix of journal bearings (i = 3 or 4) \ symmetric case
F_i	static load on bearing (i = 3 or 4) [N]
$\mathbf{G}$	dimensionless gyroscopic matrix
J_a and J_d	axial and diametral moment of inertia of rotor, scaled by ml_s^2
k_{bfi}	total stiffness between bearings and frame ($i = x$ or y on planes xz or yz) [N/m]
$k_h = 0.5\times mg/c$	hydrodynamic reference stiffness [N/m]
$k_J = 48EI/l_s^3$	stiffness of Jeffcott rotor [N/m]
$\mathbf{k}_{jbi}$ \ $\mathbf{k}_{jb}$	physical stiffness matrix of journals bearing, (i = 3 or 4) \ symmetric case [N/m]
$\mathbf{k}_s$	shaft stiffness matrix [N/m, N, Nm], [force, moments]/[displacements, rotations]
$\mathbf{K}$	total dimensionless stiffness matrix
$K_{bfi} = k_{bfi}/k_h$	total dimensionless stiffness between bearings and frame ($i = x$ or y)
$\mathbf{K}_{jbi} = \mathbf{k}_{jbi}/k_h$ \ $\mathbf{K}_{jb}$	dimensionless stiffness matrix of journal bearing (i = 3 or 4) \ symmetric case
K_{kc}	dimensionless parameter (2nd parag. of Sect. 3)
l_s, l_3, l_4 \ $L_i = l_i/l_s$	lengths of shaft and shaft branches [m] \ dimensionless lengths
m	rotor mass [kg]
$\mathbf{M}$	dimensionless mass matrix
$S_{modified}$	modified Sommerfeld number, defined by equation (3)
s_i \ $S_i = s_i/k_h$	stiffness parameters of shaft branches [N/m] \ dimensionless parameters
t_3, t_4 \ $T_i = t_i/l_s$	distances of rotor mass centre from rotor ends [m] \ dimensionless distances

$\mathbf{u}$, $\mathbf{v}$, $\mathbf{w}$	displacement vectors of rotor, journals and bearings (5th parag. of Sect. 2) [m, rad]
$\mathbf{u}_s$, $\mathbf{v}_s$	displacement vectors of rotor and journals (3rd parag. of Sect. 2) [m, rad]
$\mathbf{U}$, $\mathbf{V}$, $\mathbf{W}$	dimensionless displacement vectors (10th parag. of Sect. 2)
U_{rb}, V_{rb}, U_{rj}, V_{rj}	dimensionless displacements of bearings and journals for conical motions
U_{tb}, V_{tb}, U_{tj}, V_{tj}	dimensionless displacements of bearings and journals for cylindrical motions
Γ	dimensionless characteristic number for pure imaginary roots of $E(\Lambda) = 0$
ε_i	dimensionless eccentricity of journal bearings (i = 3, 4)
$\theta = \omega t$	dimensionless time variable
$\lambda \setminus \Lambda = \lambda/\omega_0$	characteristic number [1/s] \ dimensionless characteristic number
$\Delta\varphi$, $\Delta\psi$	tilt angles of rotor around x and y
ω	rotor angular speed [1/s]
$\omega_0 = \sqrt{k_h/m}$	reference circular frequency [1/s]
$\Omega = \omega/\omega_0$	dimensionless angular speed

References

[1] Childs D 1993 *Turbomachinery Rotordynamics* (New York: J. Wiley & S.)
[2] Rao JS 1996 *Rotor Dynamics* (New Delhi: New Age International)
[3] Lund JW 1965 Rotor bearings dynamic design technology, part III (*Design Hand Book for Fluid Film Bearings* , Mechanical Technology Inc., AFAPL-Tr-65-45)
[4] Luneno JC and Aidanpää JO 2010 Use of nonlinear journal-bearing impedance description to evaluate linear analysis of the steady-state imbalance response for a rigid symmetric rotor supported by two identical finite length hydrodynamic journal bearings at high eccentricities (*Nonlinear Dynamics* vol 62) pp 151-165
[5] Sawicki JT and Rao TVVLN 2004 A nonlinear model for the prediction of dynamic coefficients in a hydrodynamic journal bearing (*Intern. J. of Rotating Machines* vol 10) pp 507-513
[6] Qiu ZL and Tien AK 1997 Identification of sixteen force coefficients of two journal bearings from impulse responses (*Wear* 212) pp 206-212
[7] Meruane V and Pascual R 2008 Identification of nonlinear dynamic coefficients in plain journal bearings (*Tribology International* vol 41) pp 743-754
[8] Chasalevris A and Papadopoulos C 2014 A novel semi-analytical method for the dynamics of nonlinear rotor-bearing systems (*Mechanism and Machine Theory* vol 72) pp 39-59
[9] Kiciński J and Zywica G 2014 *Steam Microturbines in Distributed Cogeneration* (Springer)
[10] Li W, Yang Y, Sheng D and Chen J 2011 A novel nonlinear model of rotor/bearing/seal system and numerical analysis (*Mechanism and Machine Theory* vol 46) pp 618-631
[11] Gunter EI Jr. and Trumpler PR 1969 The influence of internal friction on the stability of high speed rotors with anisotropic supports (*Journal of Engineering for Industry* vol 91) pp 1105-13.
[12] Newkirk BL 1924 Shaft whipping (*General Electric Review* vol 27) pp 169-178
[13] Sorge F 2015 Stability analysis of rotor whirl under nonlinear internal friction by a general averaging approach (*Journal of Vibration and Control*, DOI: 10.1177/1077546315583752).
[14] Nicholas JC and Allaire PE 1978 Analysis of step journal bearings – finite length, stability (*ASLE Transactions* vol 22) pp 197-207